



Unprecedented Synthesis of Silver Nanoparticles (AgNPs) Employing Synergistic Action of Novel Ionic Liquid 1-N-(ferrocenylmethyl)-3-octylimidazolium bromide (FcMeOIMIBr) and *Launaea Oleracea* (Sarmentosa) Plant extract and their Biological Evaluation

S. J. Kamble^{1*}, P. A. Bansode², K. D. Pawar³, P. D. Kamble⁴, K. D. Sonawane⁵, G. S. Kamble⁶, J. M. Patil^{7*}

¹Sanjay Ghodawat Polytechnic, Atigre, Maharashtra, India. 416118.

²Department of Chemistry, Sangola College Sangola, Maharashtra, India. 413307.

³School of Nanoscience and Nanotechnology, Shivaji University, Kolhapur, Maharashtra, India. 416004.

⁴Balasaheb Desai College, Patan, Maharashtra, India. 415206.

⁵Department of Biochemistry, Shivaji University Kolhapur, Maharashtra, 416004.

⁶Department of Engineering Chemistry, Kolhapur Institute of Technology's College of Engineering (Autonomous), Kolhapur, Maharashtra, India. 416004.

^{7*}D.K.T.E. Society's, Textiles and Engineering Institute, Ichalkaranji, Maharashtra, India. 416115.

Abstract:

Silver nanoparticles (AgNPs) have been synthesized under the synergistic action of novel ionic liquid 1-N-(ferrocenylmethyl)-3-octylimidazolium bromide (FcMeOIMIBr) along with *Launaea Oleracea* (Sarmentosa) leaf extract. The synthesized AgNPs were confirmed by the change in colour of leaf extract and with the help of UV-vis absorbance spectra. The typical absorption peak at 437nm indicates that there are AgNPs. The synthesized AgNPs were optimized by all the reaction parameters like concentration of salt solution of silver, pH of the extract, extract and precursor ratio, temperature of the reaction and time of the reaction. The powdered AgNPs were characterized by DLS, XRD, FTIR, TEM, and EDAX in order to study their size, morphology, crystalline nature and elemental composition. The synthesized nanoparticles were evaluated for their potential biological applications and found to display promising antibacterial, antifungal and antioxidant activity.

Keywords: *Launaea Oleracea* (Sarmentosa), Ionic liquid, Biogenic silver nanoparticles, XRD, FTIR, TEM, EDAX, antibacterial activity, antifungal, antioxidant activity, gram positive, gram negative

*Corresponding Author: S. J. Kamble, Email: sachin.kamble305@gmail.com

1. Introduction:

Nanoscience and nanotechnology are the interdisciplinary branches dealing widely with the synthesis of metal nanoparticles and a large range of composite nanomaterials for their immense

commercial use in various fields. The natural sciences like physics, chemistry, biology and their other sub branches like material science, health science and engineering together form the 'Nanoscience and Nanotechnology' interdisciplinary branch. This branch focuses on the synthesis of nanoparticles, and its potential involvement in various fields such as antibacterial and antioxidant activity against many degenerative diseases like cancer [1, 2]. Since last decades, the importance of nanoscience and nanotechnology has been increased not only in the field of biology and it is well recognized today by the researchers from all sectors worldwide. Many more physical and chemical methods have been suggested for the synthesis of nanoparticles and nano-composites of desired properties. These methods can be done in a short period of time. The methods are capable of demonstrating new properties with shape and size [3]. These methods involve CBD, Vapor deposition, Lithography, sol-gel, ultrasonic fields, thermal process, photochemical reduction, sputtering and chemical etching.[4-9]. But these methods are costlier and are worst affecting on environment as it involves usage of non-degradable chemical reducing agents. To overcome these issues, a bio-green and clean method is needed to synthesize nanoparticles which include ionic liquids and plant extracts rather than harmful chemical reducing agents. This has spurred a great interest in the development of new eco-benign methods based on the use of plant extract and ionic liquid for green synthesis of nanoparticles. Nano-biotechnology deals mainly with systems of green production of nano composites and nanomaterials and their potential applications in the diverse fields of life sciences.

The green synthetic approach for biologically active AgNPs focuses on application of plant extract and ionic liquids. The reduction and stabilizing the process is done by biomolecules which exist in plant extract.[10]. The as-synthesized AgNPs offers a greater surface to volume ratio so as they are implemented in various fields such as drug delivery [11], hazardous dye degradation [12] antimicrobial property[13], Bio-mimicking, nano-sensing, super hydrophobicity [14], catalysis[15], anticorrosion, bio-fertilizer[16, 17].

The nanoparticles prepared by use of microorganisms take much time duration for its maintenance, [18-20] but the synthesis using plant extracts and ionic liquids consumes lesser time for the processing. The bio-reductive properties of extracts of leaves of some of the selected plants like *Anethum graveolens*, *Malva parviflora*, *Allium kurrat*, *Beta vulgaris sub sp. Vulgaris*, and *Capsicum frutescens* is been reported by Mervat et al. [21]. It was found that the synthesis of nanoparticles using *Malva parviflora* was effectively bioactive, monodispersed and stable. The plants with ayurvedic characters like *Camellia sinensis* [22], *Azadirachta indica* (neem) leaf extract [23] *Aloevera* [24] and latex of *Jatropha curcas* [25] etc. were also showed a better result in the

production of nanoparticles. Techniques of fabricating silver nanoparticles have become researchers' favorite field as it is one of the most important metals used globally. As silver shows a good antimicrobial action [26], it's been used for preserving drinkable and eatable items from ancient period. Synthesis of silver metal nanoparticles has gained more focus as it has a very important role in retarding the growth of microorganisms in biological systems [27] and in catalysis among other metals. As an antimicrobial agent silver has attained more attention due to its microbe resistant activity [28, 29]. Many reports are available showing synthesis of silver nanoparticles through physical and chemical routes [30, 31] with desirable shape and size having the property of antimicrobial activity but its effective practice in biomedical arena is undefined due to its toxicity. The potential antimicrobial activity of silver nanoparticles has boundless importance and has been explored in number of medical processes and industrial applications. [32] Commercially, it is prepared on bulk scale and broadly used as an anti-microbial agent in making lotions, creams and ointments to cure wounds and infections [33]. Due to variable shapes and sizes of silver nanoparticles shown different optical, mechanical, electrical and structural properties. The surface area silver nanoparticles are comparatively more than the original bulk silver. As synthesis of silver nanoparticles using biological route is cheap, simple and eco-friendly the present study deals with bio-green synthesis of silver NPs with novel ionic liquid 1-N-(ferrocenylmethyl)-3-octylimidazolium bromide (FcMeOIMIBr) and aqueous *Launaea Oleracea* (Sarmentosa) leaf extract for bio-reduction and conversion of Ag^+ to Ag^0 . Stabilization and capping of prepared nanoparticles is also performed by the synergistic action of (FcMeOIMIBr) and *L. Oleracea* aqueous leaf extract. The work flow for biological synthesis is shown in **Fig. 1**. For studying morphology and other properties of nanoparticles the various techniques like UV-vis absorbance spectra, FTIR, XRD, TEM with SAED, and EDAX were employed. Their antibacterial, antifungal and antioxidant activity was checked for various bacterial strains.

2. Experimental Details:

2.1 General

All reagents and solvents were purchased from commercial sources and used without further purification. Analytical thin layer chromatography (TLC) was performed on precoated silica gel 60F 254 plates and spots were visualized under UV light. FT-IR spectra were measured with a Perkin Elmer One FT-IR spectrophotometer. The samples were examined as KBr discs ~5% w/w. ¹H NMR and ¹³C NMR spectra were recorded on Bruker AC 400/100 MHz NMR spectrometer in CDCl₃ as solvent and tetramethylsilane (TMS) as an internal standard. Mass spectra were recorded with a Shimadzu QP2010 GC-MS. Elemental analyses were performed in a Perkin-Elmer PE 2400, Series II, CHNS/O analyser. Melting points were determined using MEL-TEMP capillary melting point apparatus and are uncorrected. Precoated aluminium sheets (silica gel 60 F254) were used for thin-layer chromatography (TLC). Column chromatography was performed on silica gel (60-120 mesh) using ethyl acetate/petroleum ether. 1-N-(ferrocenylmethyl) imidazole (3) was synthesized according to reported literature procedure[34]

2.2. Synthesis of 1-N-(ferrocenylmethyl)-3-octylimidazolium bromide (FcMeOIMIBr)

A mixture of 1-N-(ferrocenylmethyl) imidazole (1 mmol) and octyl bromide (1 mmol) was taken in acetonitrile (5 ml) in a round bottom flask. The reaction mixture was stirred at ambient temperature. After completion of reaction as monitored by thin layer chromatography (TLC), a large volume of diethyl ether was added to form crystals. The resultant crude resultant ionic liquid was isolated by column chromatography on silica gel (mesh 60-120) using pet ether/ethyl acetate as eluent (8:2 v/v).

2.3 Preparation of *Launaea Oleracea* (Sarmentosa) Leaf extract and Synthesis of AgNPs:

Launaea Oleracea (Sarmentosa) leaves were obtained from local farm of the village Atigre, Maharashtra. To obtain extract, *Launaea Oleracea* (Sarmentosa) leaves were weighed 5 gm accurately, then they were cleaned thoroughly with sterile DDW then those were chopped into fine pieces and boiled in 50 ml of DDW at 80°C for 5 min in a conical flask. The extract was sieved and the filtrate thereafter obtained was kept at 4°C in refrigerator for the further use. Silver nitrate (AgNO₃) as a precursor was obtained from Sigma Aldrich and used as it is without any further purification. In order to synthesize silver nanoparticles, 1 ml of extract is added to the 100 ml of 0.01 M AgNO₃ with constant stirring. The bio-reduction of Ag⁺ ions is monitored using UV-vis spectrometer.

2.4. Optimization of synthesis of AgNPs:

Silver nitrate (AgNO_3 , A.R. 99.9%; HiMedia, Mumbai, India) was used as a pre-cursor for synthesis of AgNPs. *Launaea Oleracea* (*Sarmentosa*) leaf extract and 1-N-(ferrocenylmethyl)-3-octylimidazolium bromide (FcMeOIMIBr) were added to solution of AgNO_3 (precursor with different concentrations (0.001–0.1M), with various Extract and ionic liquid to Precursor ratios as 1:1–1:4 (v/v) in Erlenmeyer flask with constant stirring. An aseptic condition is maintained during this process. 1 M NaOH was used to optimize the pH and pH range kept varied from 5 to 10. Reaction temperature was kept in between room temperature to 80°C . The reaction mixture was then optimized for its time parameter which was maintained and observed between 2 h to 24 hrs. During this entire parameter optimizing process, there observed a change in colour which confirms the bio-reduction of Ag ions to which was monitored by recording UV–VIS spectrum. The AgNPs from the reaction mixture was isolated by centrifugation at 12000 rpm for 10 minutes. After centrifugation; the supernatant was discarded carefully to collect the Ag_NPs that was washed 5–6 times with sterile distilled deionized water (SDDW) and allowed for drying at 60°C for 12hrs.

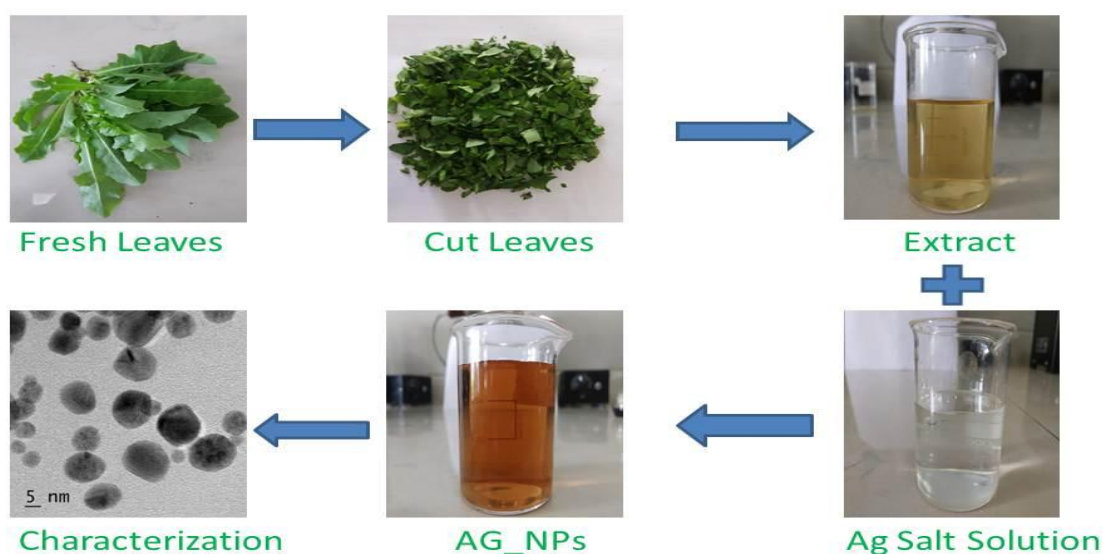


Fig.1. Work Flow for Biological synthesis of Ag_NPs using leaf extract and 1-N-(ferrocenylmethyl)-3-octylimidazolium bromide (FcMeOIMIBr)

2.5. Characterization of biogenic Ag_NPs:

The morphological characteristics and various physical properties of Ag_NPs were studied with the help of different spectroscopic techniques. The conversion of Ag^+ ion into Ag_NPs was monitored using UV–VIS (BioSpectrometer (Eppendorf, Hamburg, Germany). absorbance spectra. The wavelength range for this was opted between 250 and 800 nm. Fourier Transform Infra-Red (FT-IR) spectroscopy (Shimadzu, Japan) was used to identify the functional groups on biosynthesized Ag_NPs. The elements with their compositions were identified by EDAX spectrometer technique using x-act with INCA® and AZtec® EDS analysis software (Oxford Instruments, UK). With the help of X-ray diffraction pattern (XRD, Bruker AXS Analytical Instruments Pvt. Ltd., Germany) obtained the crystalline nature of AgNPs studied. Transmission Electron Microscope (TEM) with Selected Area Electron Diffraction pattern (SAED) is used to study the shape, the size and morphology of synthesized nanoparticles.

2.6. Ag_NPs as an Anti-microbial activity agent:

Agar well diffusion assay which is reported by Perez et al. [35] was followed as an assay for the anti-microbial study of biogenic AgNPs against some of the photogenic bacteria such as Gram-positive *Staphylococcus aureus* (NCIM 2654), Gram negative *Proteus vulgaris* (NCIM 5266) and fungus *Candida albicans* (NCIM 3557). These organisms were obtained from Microbiology Department of Shivaji University, Kolhapur, Maharashtra, India. Agar Well diffusion assay was used to check the antimicrobial activity of synthesized compound against bacterial and fungal strain.

2.7. Preparation of samples:

Stock solutions with concentration of 1 mg mL^{-1} of the as-synthesized NPs were prepared using sterile Mili-Q water. The agar plate wells were loaded with the test sample with various concentrations (25 μl , 50 μl , and 100 μl). Plates were spread with the respective organisms under test to determine its anti-microbial potential of nanoparticles. The plates were kept incubated for 24 h at 37 °C for the bacterial pathogens and for the fungal pathogens it is incubated at 27 °C for 48–72 h.

2.8. Antimicrobial assay:

The purified nanoparticles samples were checked for antimicrobial activities against various pathogenic microorganisms. Agar well diffusion method/assay is applied for the same. Sterile Muller Hinton (Accumix) agar plates used for Gram positive organisms like *Staphylococcus aureus* (NCIM 2654) and Gram-negative *Proteus vulgaris* (NCIM 5266) microorganisms, whereas Malt extract-Glucose-Yeast extract-Peptone (MGYP) was used for fungus *Candida albicans* (NCIM 3557). The suspension of test organisms was spread over agar plates aseptically, and then wells with diameter of 0.7 cm were bored aseptically and filled with the sample substance. Thereafter, these plates were preserved at 4 °C for 10 min and then allowed them for incubation at 37 °C for 24 h. After 24 h of incubation time, the plates were observed for zones of inhibition.

3. Results and Discussions:

3.1.1 Synthesis and Spectral data for 1-N-(ferrocenylmethyl)-3-octylimidazolium bromide

A prototype reaction was carried out which involved quaternization of 1-N-(ferrocenylmethyl)imidazole with 1-bromo octane in dry acetonitrile for 24 hours. After completion of the quaternization reaction as monitored by TLC, a large volume of diethyl ether was added slowly to form separate layers. After 48 h, crystals obtained from acetonitrile layer were collected by filtration to afford a yellowish-brown IL containing 1-N-(ferrocenylmethyl)-3-octylimidazolium bromide (Scheme 1) which was subjected to spectral analysis. The spectral data is in good agreement with the proposed structure.

Scheme 1. Synthesis of 1-N-(ferrocenylmethyl)-3-octylimidazolium bromide

3.1.2 Spectral data for 1-N-(ferrocenylmethyl)-3-octylimidazolium bromide

Yellow solid (340 mg, 74 %); mp 78-80 °C. FTIR (KBr) ν (cm⁻¹): 2921, 1638, 1546, 1475, 1399, 1265, 1139, 1109, 1087; ¹H NMR (CDCl₃, 400 MHz): δ 7.77 (d, J = 8.1 Hz, 2H), 7.24 (d, J = 8.1 Hz, 2H), 6.57 (dd, J = 12, 12 Hz, 1H), 5.66 (d, J = 12.3 Hz, 1H), 5.52 (d, J = 18 Hz, 1H), 3.44-3.39 (m, 2H), 3.34-3.29 (m, 2H), 2.39 (s, 3H), 1.60-1.40 (m, 4H), 1.34-1.22 (m, 4H), 0.93-0.88 (m, 6H)

ppm; ^{13}C NMR (CDCl_3 , 100 MHz): δ 164.1, 141.5, 129.0, 128.8, 126.3, 123.8, 49.8, 47.9, 30.5, 28.8, 21.4, 20.1, 19.8, 13.6 ppm; Anal. Calc. for $\text{C}_{22}\text{H}_{31}\text{N}_2\text{FeBr}$: % C 57.54, % H 6.80, % N 4.72, % Fe 12.16, % Br 17.40 Found: % C 57.46, % H 6.68, % N 4.66, % Fe 12.09 % Br 17.34.

3.2.1. UV-Visible Spectral Analysis:

On addition of measured quantity of extract to the Ag salt solution the mixture began to turn brown coloured from transparent light-yellow colour. This change in colour is because of the excitation that takes place in surface Plasmon vibrations and this is the clear indication of the formation of Ag_NPs. The bio-reduction process of Ag^+ to Ag^0 metal nanoparticles in this process is monitored by UV-Visible spectral analysis in the range between 250nm to 800nm. The colloidal solution obtained was centrifuged at 12000 rpm to isolate Ag_NPs. The insoluble greyish-black coloured powder was obtained after this centrifugation reaction. In a bath sonicator, it was sonicated for 20 to 30 min to get well dispersion in water. The free electrons associated with the nanoparticles yield a SPR absorption band. This is because of a resonance that takes place between electrons of nanoparticles and light wave. As a characteristic of surface plasmon resonance (SPR) of silver nanoparticles there is appearance peak. The maximum absorption (**Fig. 2**) is obtained at 415 nm which indicates that, the successful synthesis of Ag_NPs with environmental green synthesis method.

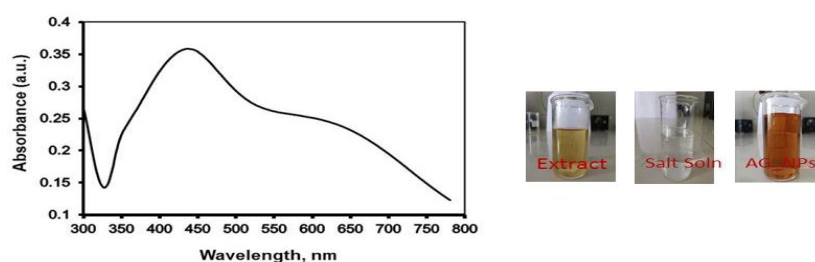


Fig. 2. UV-Vis absorbance spectrum of biogenic synthesis of Ag_NPs

3.2.2. X-Ray Diffraction Studies (XRD):

The XRD technique was implemented to study the crystal nature and structure of synthesized Ag_NPs. It was studied by plotting a XRD pattern using $\text{Cu K}\alpha$ radiation ($\lambda = 1.54184 \text{ \AA}$) in 2θ with

the range 10° to 100° (scan speed $3^{\circ}/\text{min}$). **Fig.3** shows the XRD pattern of Ag_NPs. The XRD pattern shows the Bragg reflections at 2θ values of 31.52° , 38.24° , 44.43° , 64.17° , and 77.52° representing (101), (111), (200), (220), and (311) planes, respectively. The XRD patterns were consistent and matched with the database of JCPDS card No.040783. It reveals that the as-synthesized Ag_NPs are crystalline with face centered cubic (FCC) structure. The observed XRD data well matches with previous reports(26-29).The crystallite size has been calculated by using of well-known Debye–Scherer’s equation $D=0.9\lambda/\beta\cos\theta$. And the average crystallite size of Ag_NPs is 24.86 nm.

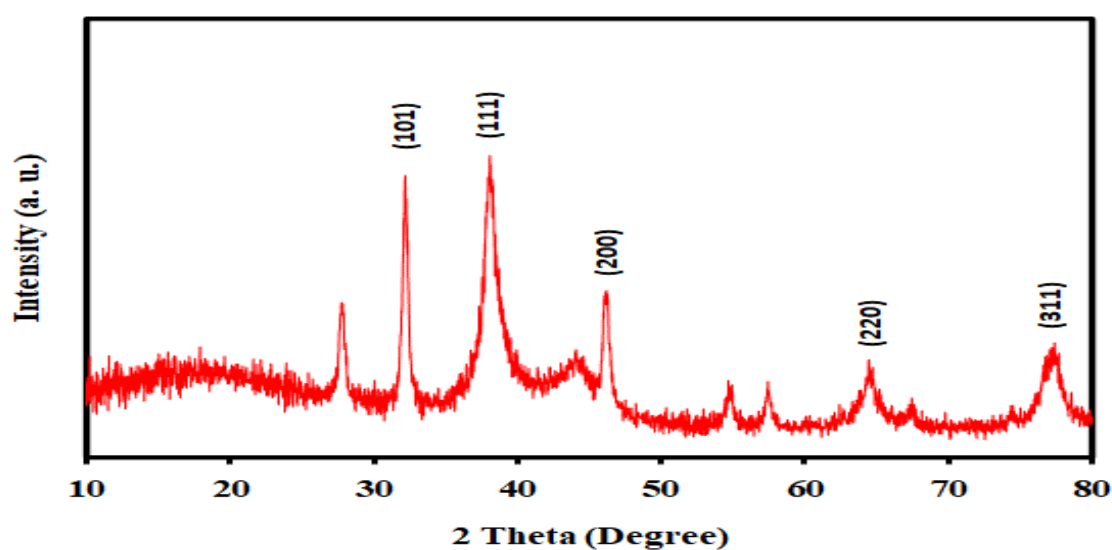


Fig. 3. XRD pattern of crystalline as-synthesized AgNPs

3.2.3. Fourier Transmission Infra-Red Studies:

The FTIR spectral analysis were recorded to identify the biomolecule which could have been responsible for the bio-reduction of Ag^+ to Ag^0 NPs during synthesis and to identify the possible functional group/s on bio-molecule involved in bio-reduction and the stability of Ag_NPs. The FTIR analysis (**Fig. 4**) revealed the strong bands at 3432.67 , 2922.57 , 1601.59 , 1383.68 and 1021.12 cm^{-1} . A very broad absorption and strong band was found at 3432.67 cm^{-1} which indicates that the synthesized NPs could have been present the vibrations of symmetric stretching due to presence of primary amine; the asymmetric and symmetric stretching of $-\text{CH}_3$ groups were found at 2922.57 cm^{-1} and 2853.22 cm^{-1} . The absorption bands at 1601.59 cm^{-1} correlated to $\text{C}=\text{C}$ corresponds to aromatic amino groups and 1383.68 cm^{-1} were correlates the symmetric and asymmetric stretching of $-\text{COO}^-$ groups. The band at 1021 cm^{-1} which can be attributed to the $\text{C}-\text{O}$ stretching of aromatics, alcohols, aldehydes, carboxylic acids and ester groups, etc.

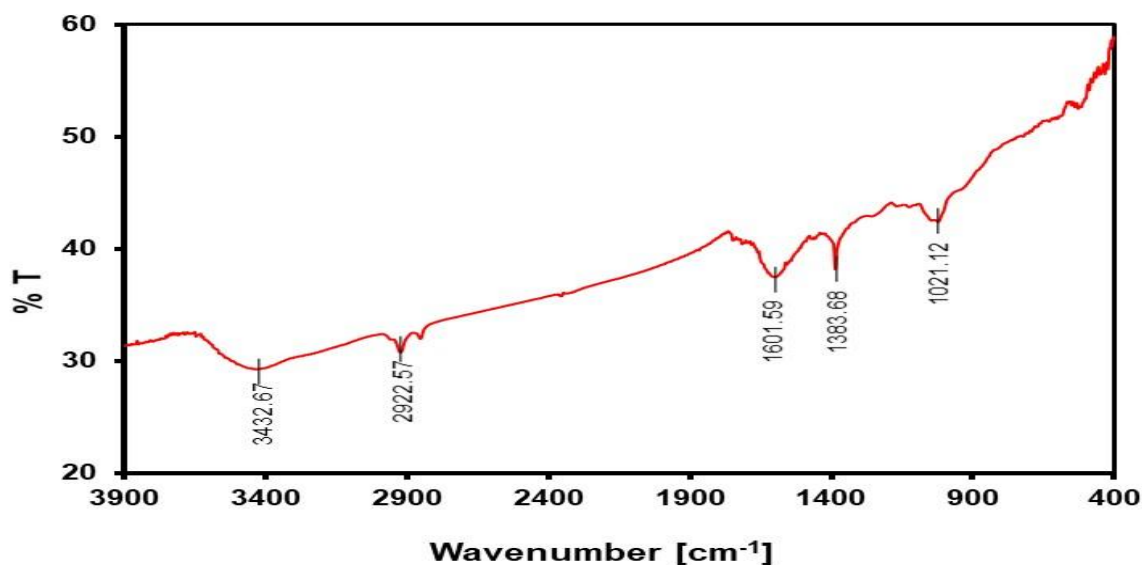


Fig. 4. FTIR spectrum of silver nanoparticles.

3.2.4. EDAX:

The synthesized powdered sample of Ag NPs was analyzed by EDAX analysis to determine the atomic and weight percentage of elemental composition. As shown in Fig. 5 mainly the Ag, O, N, Si, C and K are present in synthesized Ag NPs. The Oxygen, Carbon and Nitrogen showed peaks may be due surface capping of plant extract of flavonoids. Overall, this analysis has proved surface capping, elemental composition, purity, and particle state of Ag_NPs.

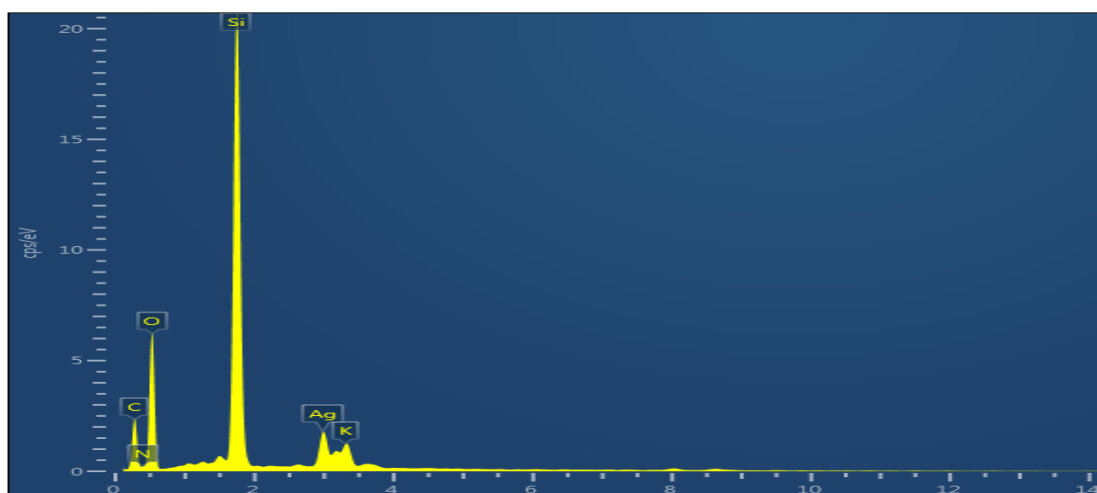


Fig. 5. EDAX graphical analysis of silver nanoparticles

3.2.5. Transmission Electron Microscopy (TEM):

This technique was mainly used to study the particle shape and size, morphology and its dispersity. The results obtained from TEM has confirmed that the synthesized Ag_NPs were mono-dispersed without any aggregation (**Fig. 6 a-d**), most of the nanoparticles are spherical in shape with size ranging between 10nm to 18nm, shown in **Fig 6c**. XRD pattern already confirmed that Ag_NPs were crystalline in nature this was further confirmed by SAED pattern. The SAED pattern of Ag_NPs have depicted the different phase arrangement which displayed five circular bright rings relating to (111), (200), (220), (311), and (222) planes which has been shown in **Fig. 6d**. The bright spots observed in the SAED pattern are indexed to face centered cubic (FCC) structure of Ag_NPs and clearly shows that synthesized Ag_NPs are crystalline in nature. There is strong resemblance between SAED pattern and XRD pattern which indicate Ag_NPs are with crystalline structure.

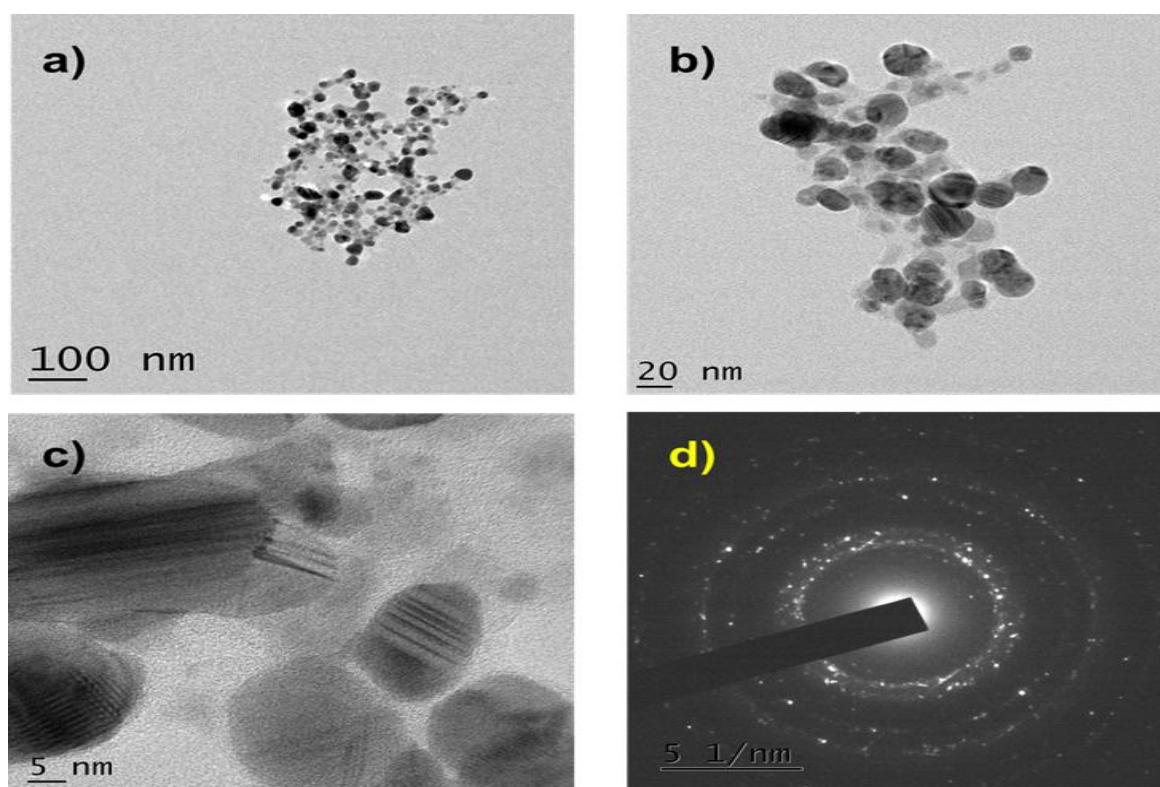


Fig. 6(a-c) TEM images, 6(d) SAED pattern of silver nanoparticles

3.2.6 Dynamic Light Scattering (DLS) with zeta potential:

Dynamic Light Scattering (DLS) was used for the measurement of average hydrodynamic diameter and poly dispersity indexes of the synthesized nanoparticles. The zeta potential of a nanoparticle represents its surface charge. It denotes the electric potential of nanoparticles, which

depends on the composition of particles as well as the dispersing medium. The hydrodynamic diameter of nanoparticles observed was 804.1 nm with polydispersity index 25.2%. Particle size distribution histogram (Fig. 7) has shown two peaks with intensities 640.8 and 54.22 nm. The zeta potential (Fig. 8) of nanoparticles was -25.9 mV with standard deviation +/- 1.2 mV. This high value for zeta potential clearly suggests that these nanoparticles are highly stable.

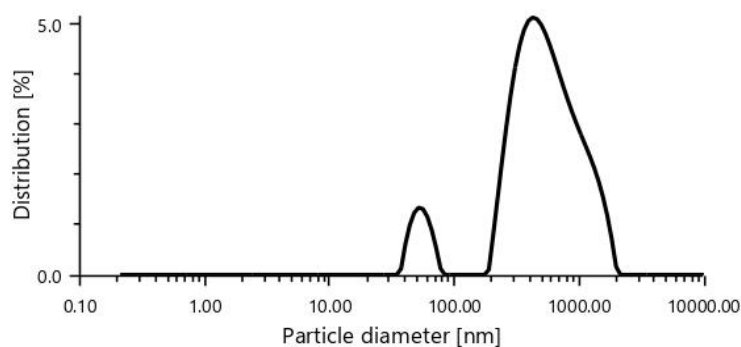


Fig. 7. Particle size distribution of AgNPs

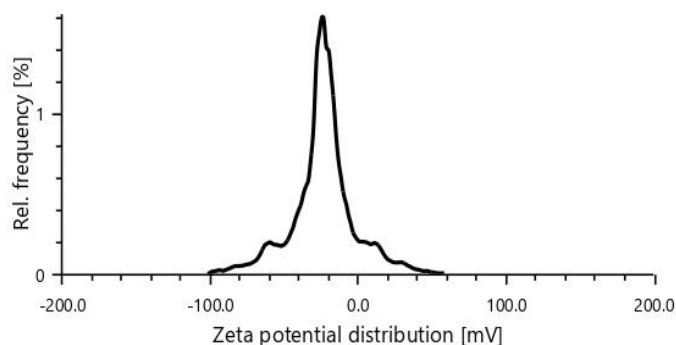


Fig. 8. Zeta potential distribution of AgNPs

3.3. Antimicrobial and Anti-oxidant activity:

3.2.7 Antibacterial and antifungal activity:

The antibacterial and antifungal studies (Table 1) have been carried out using synthesized Ag_NPs. That has shown noticeable antimicrobial activity for both Gram-positive and negative pathogens and also for antifungal activity.

In the recent years antibacterial activity of Ag_NPs is very much vital for many medical and food packing applications. The antibacterial activity [36, 37] studied against *Staphylococcus Aureus* and *Proteus vulgaris* and antifungal activity against *Candida Albicans* by using of as-synthesized

Ag_NPs. (Fig. 9 a-c). The antibacterial efficiency of Ag_NPs has been found to be enhanced because of its smaller size than the bacterial sizes. The small microbes have been got imprisoned interacted with Ag_NPs due to large surface area of it. And Ag_NPs have been creating an electrostatic attractive force between the microbial surface and Ag_NPs. The Ag_NPs interact with the microbes containing thiol groups, foremost to disturb the regular functioning of the bacterial cells and further to cause death of cell [38-40]. The antibacterial efficiency of Ag_NPs is also depends upon the shape, surface area and medium. Subsequently, due to Ag_NPs, free radicles had formed which damaged the cell membrane which results the killing of bacteria and will restricts the growth of bacteria [41-42].

Name of bacteria	Zone of Inhibition in mm		
	25µl/ml	50µl/ml	100µl/ml
<i>Staphylococcus Aureus</i>	18	19	22
<i>Proteus vulgaris</i>	14	15	14
<i>Candida Albicance</i>	15	19	23

Table1. The antibacterial and antifungal study

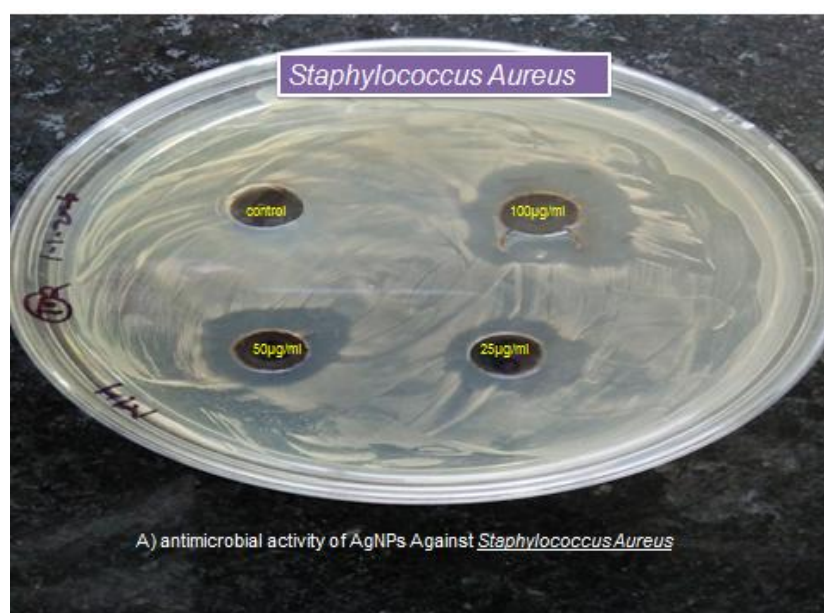


Fig. 9 a) Plate showing Antibacterial activity of Ag_NPs against *Staphylococcus Aureus*

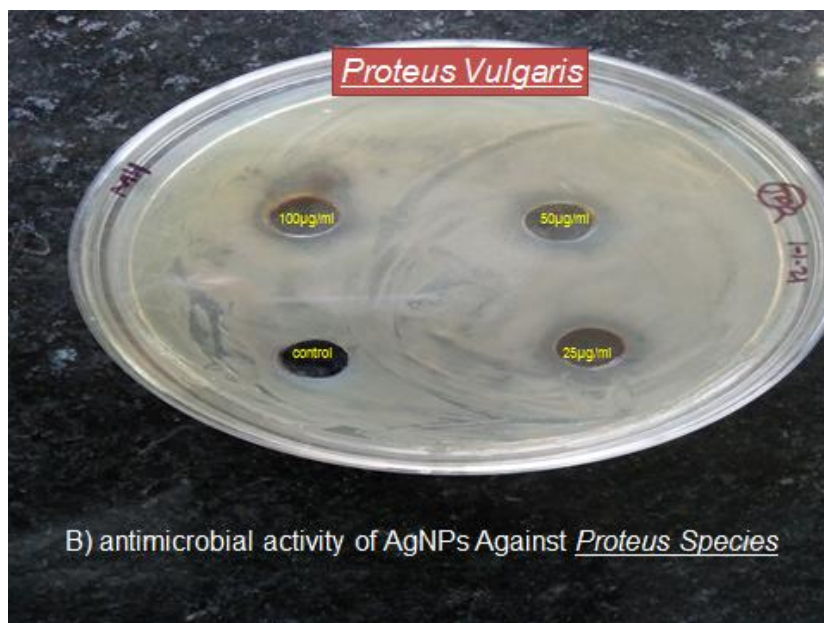


Fig. 9b) Plate showing Antibacterial activity of Ag_NPs against *Proteus vulgaris*

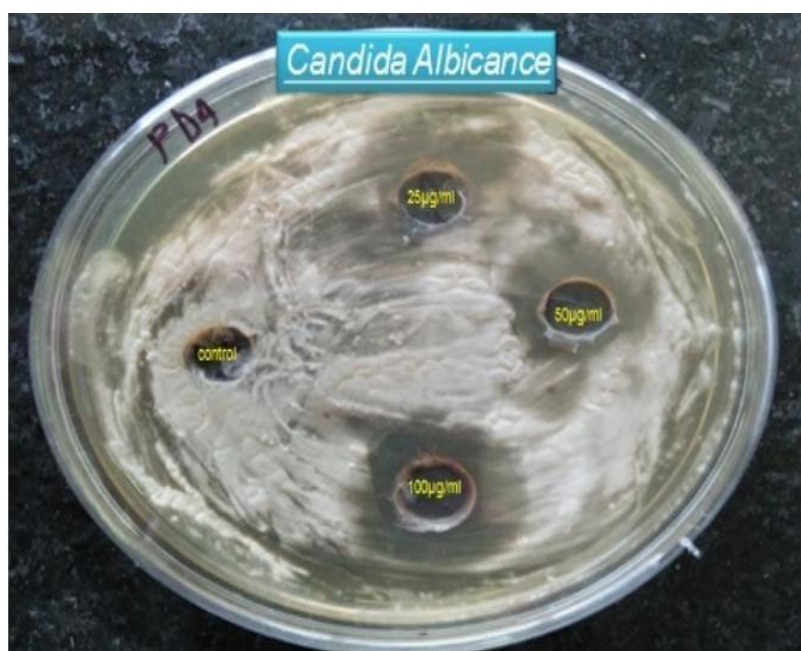


Fig. 9 c) Plate showing Antifungal activity of Ag_NPs against *Candida Albicans*

3.3.2 Antioxidant activity:

The antioxidant activity of as-synthesized Ag_NPs was assessed by using DPPH (2,2-diphenyl-1-picryl-hydrazyl-hydrate) radical scavenging assay [43, 44]. DPPH is a stable compound and it can be reduced by gaining the hydrogen or electrons. It has been extensive applications for evaluating the antioxidant activity studies. **Fig. 10** shows in-vitro antioxidant activity of bio-synthesized Ag nanoparticles from *Launaea Oleracea* (*Sarmentosa*) leaf extracts with DPPH found significant free

radical scavenging potential. The reaction mixture include 1 mL of the bio-synthesized Ag nanoparticle at various concentrations ($25\text{-}100\ \mu\text{g mL}^{-1}$) with 2 mL of $1.0\ \text{mmol L}^{-1}$ DPPH radical solution prepared in methanol, and they were incubated in the dark at $37\ ^\circ\text{C}$ for 30 minutes. The absorbance of all different mixtures was recorded using a spectrophotometer (UV-1800, Shimadzu, Japan) at 570 nm. The DPPH radical scavenging ability was calculated using the following equation.

$$\% \text{ of radical scavenging} = \frac{\text{control-sample}}{\text{control}} \times 100$$

Here all reaction mixtures with different concentrations of the bio-synthesized Ag nanoparticles displayed the good ability to scavenge free radicals in a concentration-dependent manner. Amongst the studied concentrations, the excellent scavenging activity was found for $100\ \mu\text{l}$ which scavenged $66.98 \pm 0.92\%$ of the radicals at the $10\ \mu\text{g/ml}$ concentration, it was followed by $50\ \mu\text{l}$ ($53.30 \pm 0.62\%$), $25\ \mu\text{l}$ ($26.72 \pm 1.46\%$). $25\ \mu\text{l}$ sample at $10\ \mu\text{g/ml}$ concentration showed lesser scavenging activity.

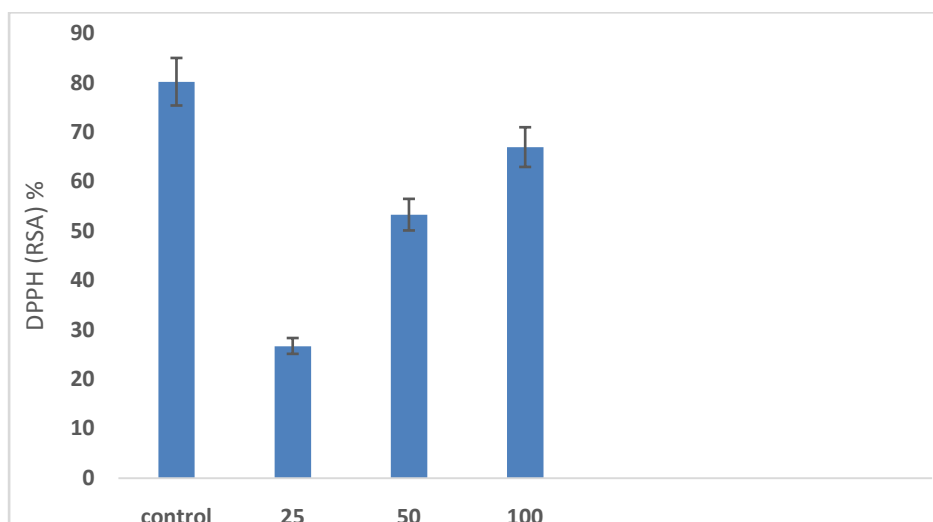


Fig. 10. Anti-oxidant activity of Ag_NPs

4. Conclusions:

The study demonstrates the unprecedented synthesis of silver nanoparticles (AgNPs) employing synergistic action of novel ionic liquid 1-N-(ferrocenylmethyl)-3-octylimidazolium bromide (FcMeOIMIBr) and *Launaea Oleracea* (*Sarmentosa*) Plant extract and their Biological Evaluation.. The developed method is cheap, bio-green and eco-friendly The formation of Ag_NPs was confirmed by UV-Vis absorption spectroscopy and also was characterized by FTIR, XRD, TEM with SAED and EDAX in order to study their shape, size, dispersity, crystalline structure,

percentage elemental composition and biomolecules responsible for bio-reduction of Ag⁺ to Ag⁰. The synthesized AgNPs demonstrated promising antibacterial, antifungal and antioxidant

Credit Author Statement

S. J. Kamble and J. M. Patil have been planned and design the experiments. All experimental work carried out by S. J. Kamble. The manuscript writing is accomplished by S. J. Kamble. Experimental results and data are examined by P. A. Bansode, K. D. Pawar, P. D. Kamble, K. D. Sonawane, G. S. Kamble and J. M. Patil.

Conflict of Interest

There are no any competing interests.

5. References:

- [1] P. Sanpui, A. Chattopadhyay, S.S. Ghosh, *Appl. Mater. Interfaces* 3 (2011) 218.
- [2] A. Nazem, G.A. Mansoori, *J. Alzheimers Dis.* 13 (2008) 199.
- [3] M. Dubey, S. Bhadauria, B.S. Kushwah, *Dig. J. Nanomater. Biostruct.* 4 (2009) 537.
- [4] F. Mafune, J. Kohoo, Y. Takeda, T. Kondow, *J. Phys. Chem. B* 106 (2002) 7575.
- [5] R.R. Naik, S.J. Stringer, G. Agarwal, S.E. Jones, M.O. Stone, *Nat. Mater.* 1 (2002) 169.
- [6] K. Okitsu, A. Yue, S. Tanabe, H. Matsumoto, Y. Yobiko, *Langmuir* 17 (2001) 7717.
- [7] T.K. Sau, A. Pal, N.R. Jana, Z.L. Wang, T. Pal, *J. Nanopart. Res.* 3(2001) 257.
- [8] W.M. Tolles, *Nanoscience and nanotechnology in Europe*, *Nanotechnology* 7 (1996) 59.
- [9] M.H. Magonnuss, K. Deepert, J. Malm, J. Bovin, L. Samuelson, *Nanostruct. Mater.* 12 (1999) 45–48.
- [10] S.V. Ganachari, N.R. Banapurmath, B. Salimath, J.S. Yaradoddi, A.S. Shettar, A.M. Hunashyal, A. Venkataraman, P. Patil, H. Shoba, G. B. Hiremath, “Synthesis Techniques for Preparation of Nanomaterials,” *Handbook of Ecomaterials*, L. M. T. Martínez, O. V. Kharissova, B. I. Kharisov, Eds., Springer International Publishing, Cham 2019, p. 83.
- [11] S. Sim, N. K. Wong, *Biomedical Reports* 2021, 14, 1.
- [12] P.D. Sarvalkar, R.R. Mandavkar, M.S. Nimbalkar, K.K. Sharma, P.S. Patil, G.S. Kamble, N.R. Prasad, *Scientific Reports* 11 (1) (2021) 16934.
- [13] A.C. Gomathi, S.R. Xavier Rajarathinam, A. Mohammed Sadiq, S. Rajeshkumar, *Journal of Drug Delivery Science and Technology* 55 (2020) 101376.
- [14] S.V. Ganachari, “Polymers for Energy Applications,” *Handbook of Ecomaterials*, L. M. T. Martínez, O. V. Kharissova, B. I. Kharisov, Eds., Springer International Publishing, Cham 2019, p. 3011.
- [15] A. Verma, M. S. Mehata, *Journal of Radiation Research and Applied Sciences* 9 (2016) 109.
- [16] S.V. Ganachari, J. S. Yaradoddi, S. B. Somappa, P. Mogre, R. P. Tapaskar, B. Salimath, A. Venkataraman, V. J. Viswanath, “Green Nanotechnology for Biomedical, Food, and Agricultural Applications,” *Handbook of Ecomaterials*, L. M. T. Martínez, O. V. Kharissova, B. I. Kharisov, Eds., Springer International Publishing, Cham 2019, p. 2681.
- [17] L.V. Hublikar, S.V. Ganachari, N. Raghavendra, V.B. Patil, N.R. Banapurmath, *Current Research in Green and Sustainable Chemistry* 4 (2021) 100212.
- [18] K.N. Thakkar, S.S. Mhatre, R.Y. Parikh, *Nanomedicine* 6 (2010) 257.

- [19] H.Bar, D.K.Bhui, G.P. Sahoo, P. Sarkar, S.P. De, A. Misra, *Colloids Surf. A Physicochem. Eng. Asp.* 339 (2009) 134.
- [20] J.Y. Song, B.S. Kim, *Bioprocess. Biosyst. Eng.* 32 (2009) 79.
- [21] F.Z. Mervat, W.H. Eisa, A.A. Shabaka, *Spectrochem. Acta. Part A* 98 (2012) 423.
- [22] A.R. Vilchis-Nestor, V. Sanchez-Mendieta, M.A. Camacho-Lopez, R.M. Gomez-Espinosa, M.A. Camacho-Lopez, J.A. Arenas-Alatorre, *Mater. Lett.* 62 (2008) 3103.
- [23] S. Shiv Shankar, A. Rai, A. Ahmad, M. Sastry, *J. Colloid Interface Sci.* 275 (2004) 502.
- [24] N.H.H. Abu Bakar, J. Ismail, M. Abu Bakar, *Mater. Chem. Phys.* 104 (2007) 276.
- [25] N. Vigneshwaran, R.P. Nachane, R.H. Balasubramanya, P.V. Varadarajan, *Carbohydr. Res.* 341 (2006) 2012.
- [26] S. Srikar, D. Giri, D. Pal, P. Mishra, S. Upadhyay, *Green Sustain. Chem.* 6 (2016) 34.
- [27] M.N. Nadagouda, G. Hoag, J. Collins, R.S. Varma, *Cryst. Growth Des.* 9 (2009) 4979.
- [28] V. Parashar, R. Parashar, B. Sharma, A.C. Pandey, *Dig. J. Nanomater Bios.* 4 (2009) 45.
- [29] A. Panaek, L. Kvitek, R. Prucek, M. Kolar, R. Veerova, N. Pizurova, V.K. Sharma, T. Nevena, R. Zboril, *J. Phys. Chem. B* 110 (2006) 16248.
- [30] V. Thirumalai Arasu, D. Prabhu, M. Soniya, *J. Biosci. Res.* 1 (2010) 259.
- [31] S. Kheybari, N. Samadi, S.V. Hosseini, A. Fazeli, M.R. Fazeli, *Daru J. Pharm. Sci.* 18 (2010) 168.
- [32] S. Ponarulselvam, C. Panneerselvam, K. Murugan, N. Aarthi, K. Kalimuthu, S. Thangamani, *Asian Pac. J. Trop. Biomed.* 2 (2012) 574.
- [33] I.P. Margaret, S.L. Lui, K.M. Vincent, I. Lung, B. Andrew, *J. Med. Microbiol.* 55 (2006) 59.
- [34] Y. Gao, B. Twamley, J.M. Shreeve, The first (ferrocenylmethyl)imidazolium and (ferrocenylmethyl)triazolium room temperature ionic liquids, *Inorg Chem.* 43 (2004) 3406-3412
- [35] P. Shukla, T. Nandi, R. Singh, *Orient. J. Chem.* 32 (2016) 2947.
- [36] R. Singh, P. Wagh, S. Wadhvani, S. Gaidhani, A. Kumbhar, J. Bellare, B. Chopade, *Int. J. Nanomed.* 8 (2013) 4277.
- [37] K. Kalimuthu, R. Suresh Babu, D. Venkataraman, M. Bilal, S. Gurunathan, *Colloids Surf. B Biointerfaces* 65 (2013) 150.
- [38] J. Singh, A.S. Dhaliwal, *Anal. Lett.* 52 (2019) 213
- [39] N.U. Islam, K. Jalil, M. Shahid, A. Rauf, N. Muhammad, A. Khan, M.R. Shah, M.A. Khan, *Arabian Journal of Chemistry* 12 (2019) 2914.
- [40] N. Raghavendra, J. Ishwara Bhat, *Journal of King Saud University - Engineering Sciences* 31 (2019) 202.

- [41] A.G. Femi-Adepoju, A.O. Dada, K.O. Otun, A.O. Adepoju, O.P. Fatoba, *Heliyon* 5 (2019), e01543.
- [42] K. Chand, M.I. Abro, U. Aftab, A.H. Shah, M.N. Lakhan, D. Cao, G. Mehdi, A.M.A. Mohamed, *RSC Adv.* 9 (2019) 17002.
- [43] G.M. Nazeruddin, N.R. Prasad, S.R. Prasad, Y.I. Shaikh, S.R. Waghmare, Parag Adhyapak, *Industrial Crops and Products.* 60 (2014) 212-216
- [44] R. Gurav, S. K. Surve, S. Babar, P. Choudhari, D. Patil, V. More, S. Sankpal and S. Hangirgekar - *Organic & Biomolecular Chemistry*, 18 (2020) 4575-4582.